Supplement of Hydrol. Earth Syst. Sci., 28, 1935–1956, 2024
https://doi.org/10.5194/hess-28-1935-2024-supplement

Hydrology and Earth System Sciences
Open Access
EGU

Supplement of

A high-resolution perspective of extreme rainfall and river flow under extreme climate change in Southeast Asia

Mugni Hadi Hariadi et al.

Correspondence to: Mugni Hadi Hariadi (mugni.hariadi@knmi.nl, mugni.hariadi@bmkg.go.id, and mugnihadi@gmail.com)

This supplementary material provides figures that are used to further illustrate the analyses and add additional detail.
S1

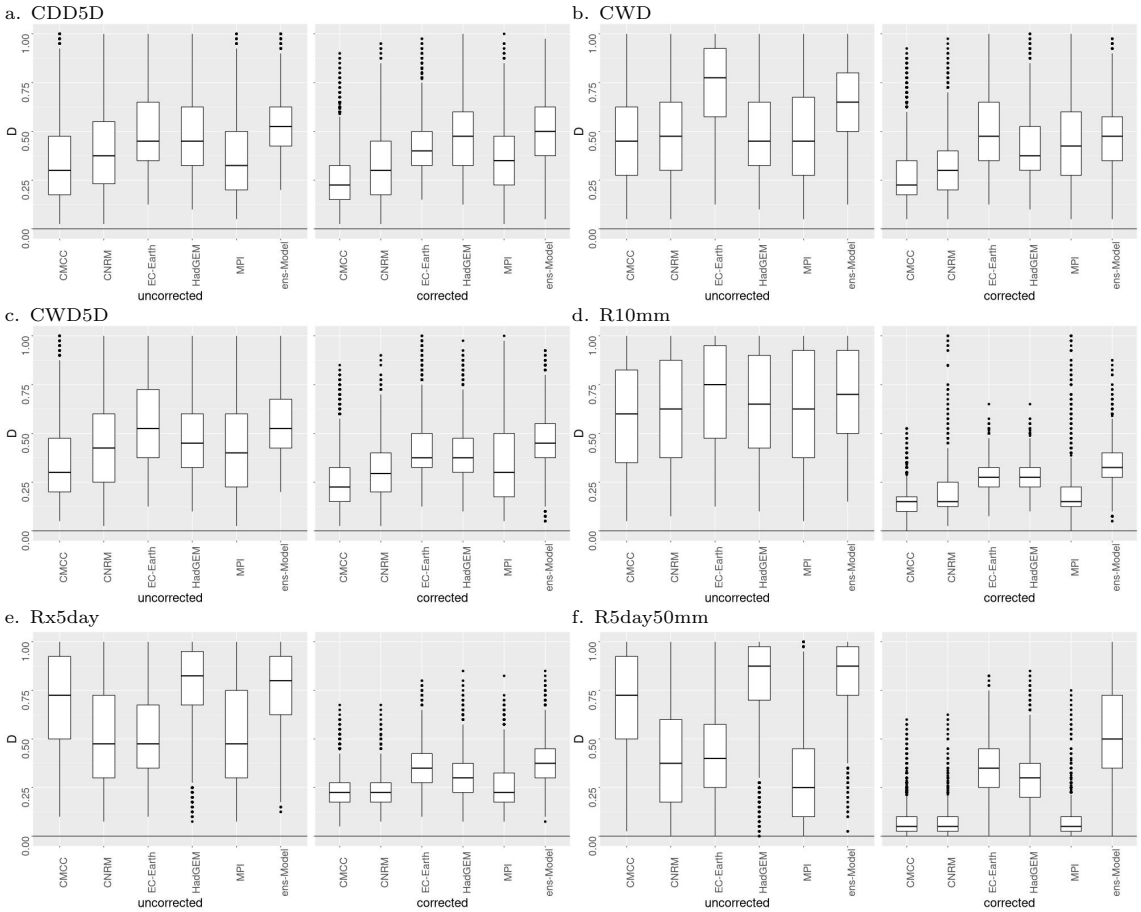

Figure S1. Supplementary Figure S01 shows the Kolmogorov–Smirnov statistic value between the original model dataset and the bias-corrected model dataset. The statistic value calculated for simulating a) CDD5D, b) CWD, c) CWD5D, d) R10mm, e) Rx5day and f) R5day50mm.

S2

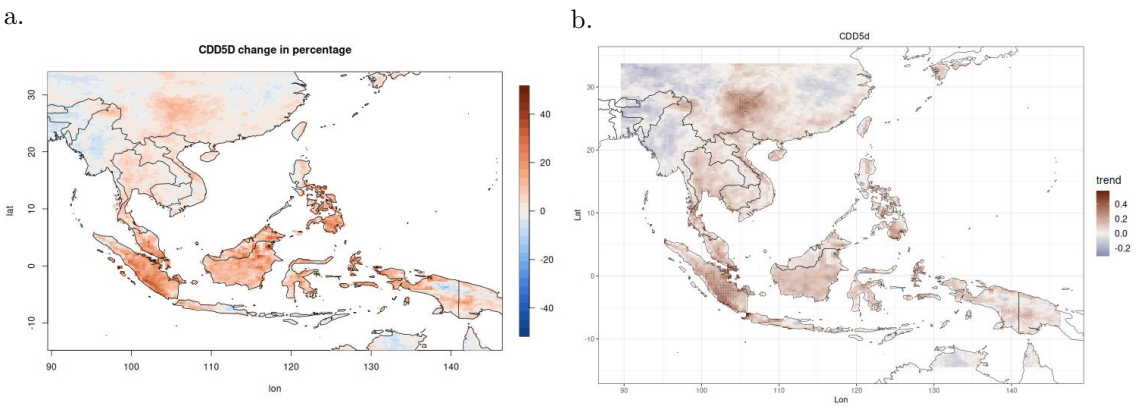

Figure S2. Annually a number of consecutive dry day periods with more than 5 days (CDD5D) change in percentage in the near future (2021-2050) compared to the historical period (1981-2010) (left), and the trend of CDD5D on the period 1971-2050 (right). The dashes in the trend map indicate model agreement in the trend significant at 60% level agreement.

S3

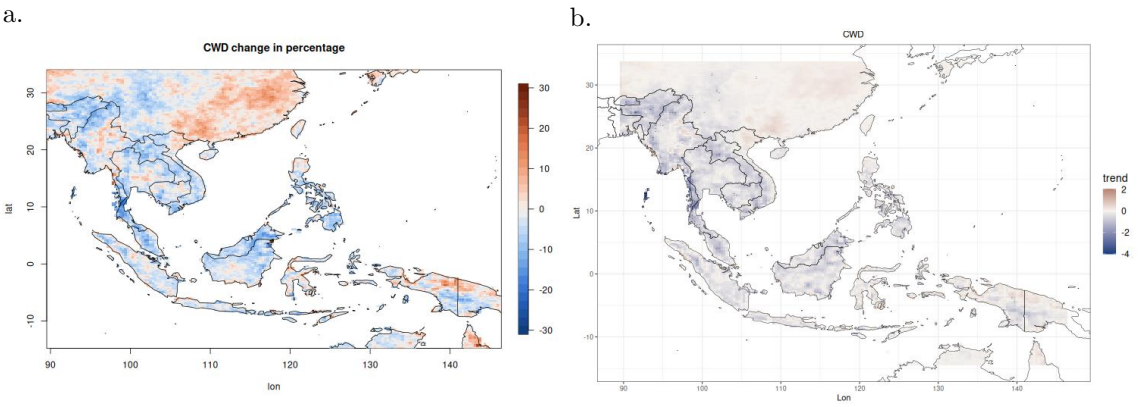

Figure S3. Annually a maximum number of consecutive wet day periods (CWD) change in percentage in the near future (2021-2050) compared to the historical period (1981-2010) (left), and the trend of CWD on the period 1971-2050 (right). The dashes in the trend map indicate model agreement in the trend significant at 60% level agreement.

S4

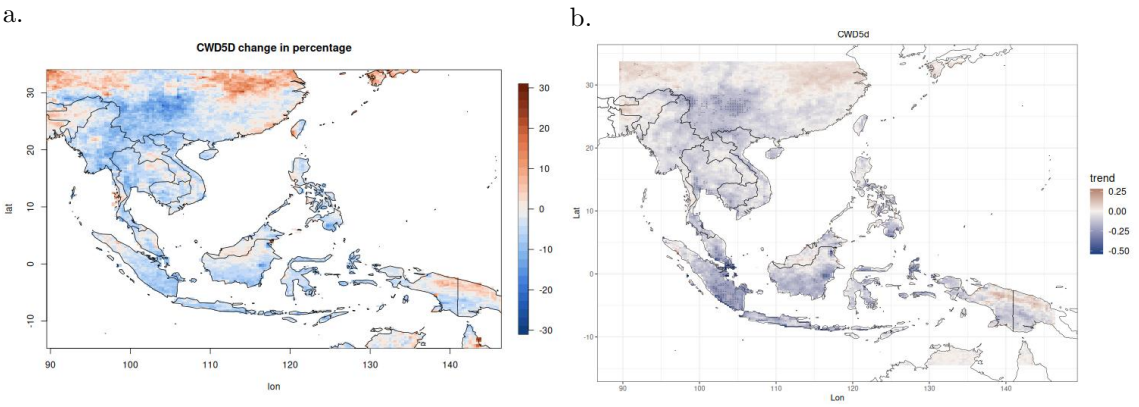

Figure S4. Annually a number of consecutive wet day periods with more than 5 days (CWD5D) change in percentage in the near future (2021-2050) compared to the historical period (1981-2010) (left), and the trend of CWD5D on the period 1971-2050 (right). The dashes in the trend map indicate model agreement in the trend significant at 60% level agreement.

S5

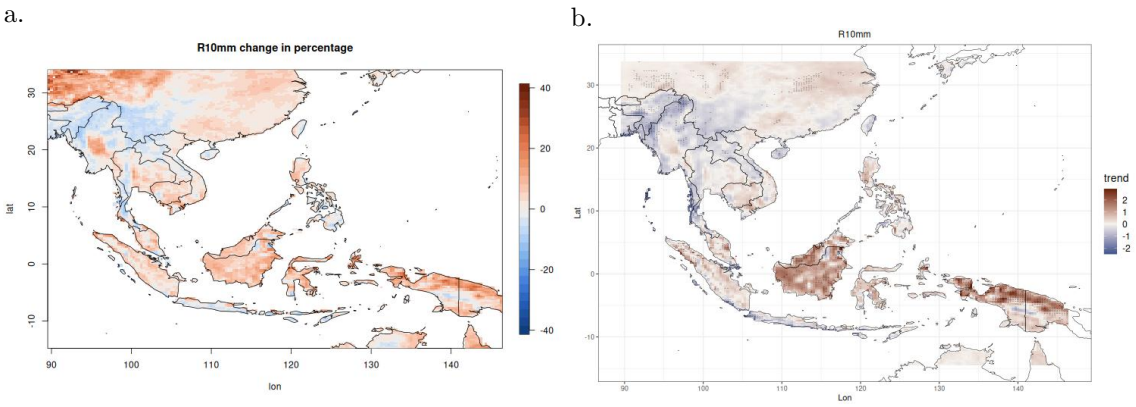

Figure S5. Annually a number of days with heavy rainfall (> 10mm) (R10mm) change in percentage in the near future (2021-2050) compared to the historical period (1981-2010) (left), and the trend of CWD5D on the period 1971-2050 (right). The dashes in the trend map indicate model agreement in the trend significant at 60% level agreement.

S6

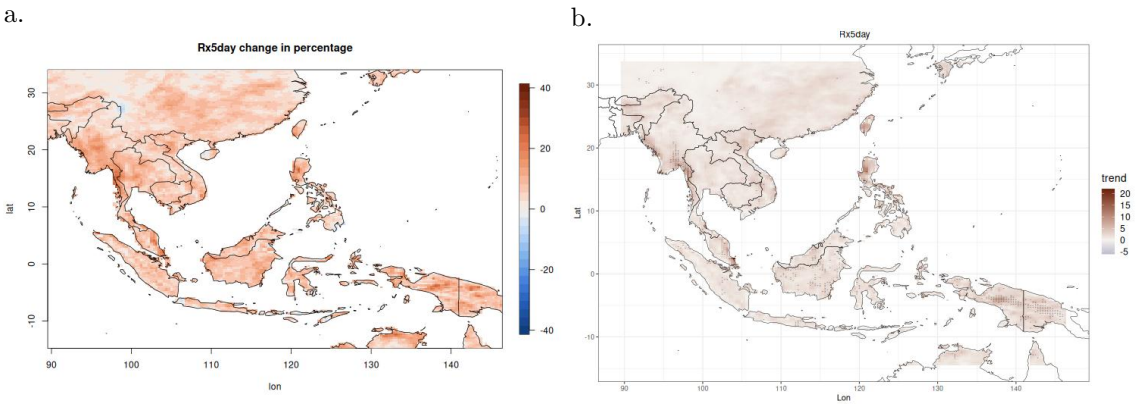

Figure S6. Annually a maximum 5-day rainfall (Rx5day) change in percentage in the near future (2021-2050) compared to the historical period (1981-2010) (left), and the trend of Rx5day on the period 1971-2050 (right). The dashes in the trend map indicate model agreement in the trend significant at 60% level agreement.

S7

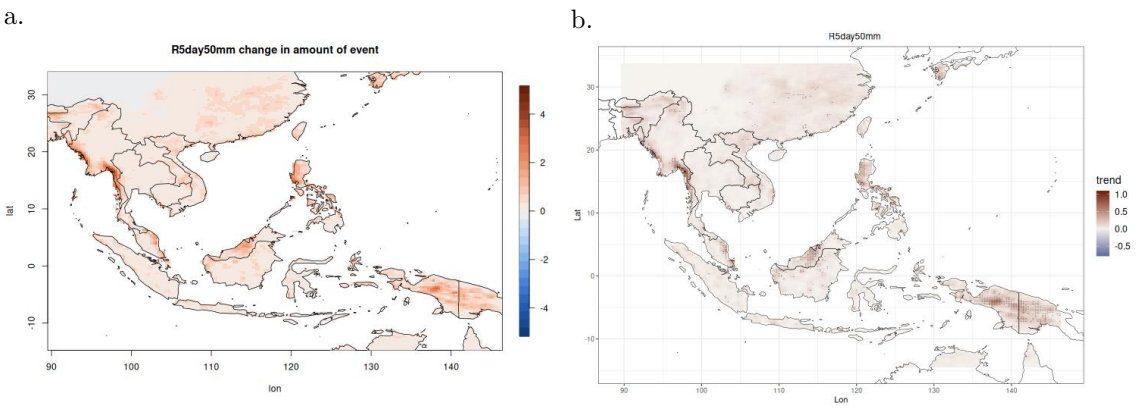

Figure S7. Annually a number of the 5-day period with cumulative rainfall >50mm (R5day50mm) change in a number of events in the near future (2021-2050) compared to the historical period (1981-2010) (left), and the trend of R5day50mm on the period 1971-2050 (right). The dashes in the trend map indicate model agreement in the trend significant at 60% level agreement.

a. DJF

b. MAM

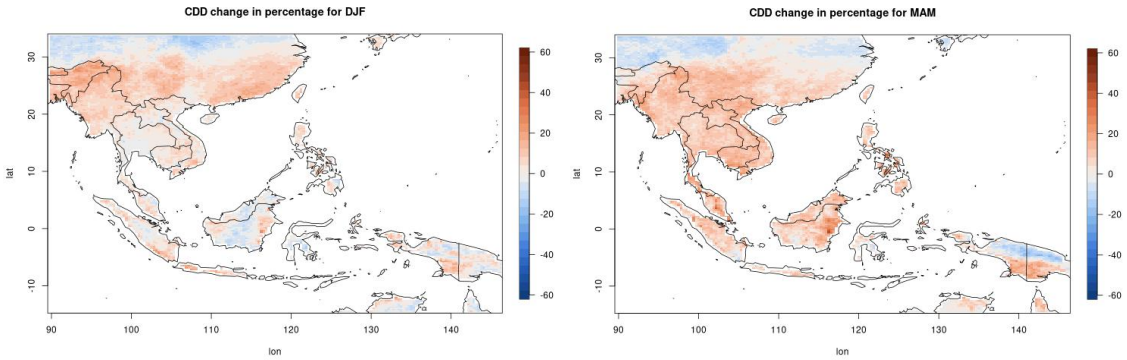

c. JJA

d. SON

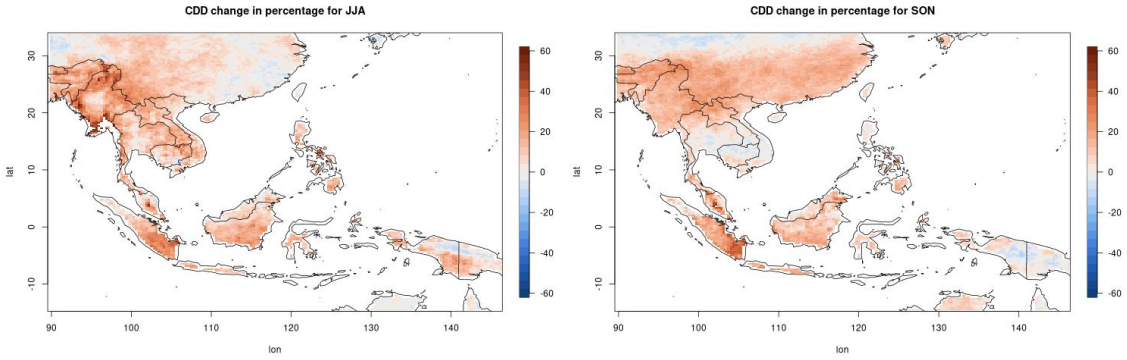

Figure S8. Seasonal maximum length of a dry spell (CDD) change in percentage in the near future (2021-2050) compared to the historical period (1981-2010).

a. DJF

b. MAM

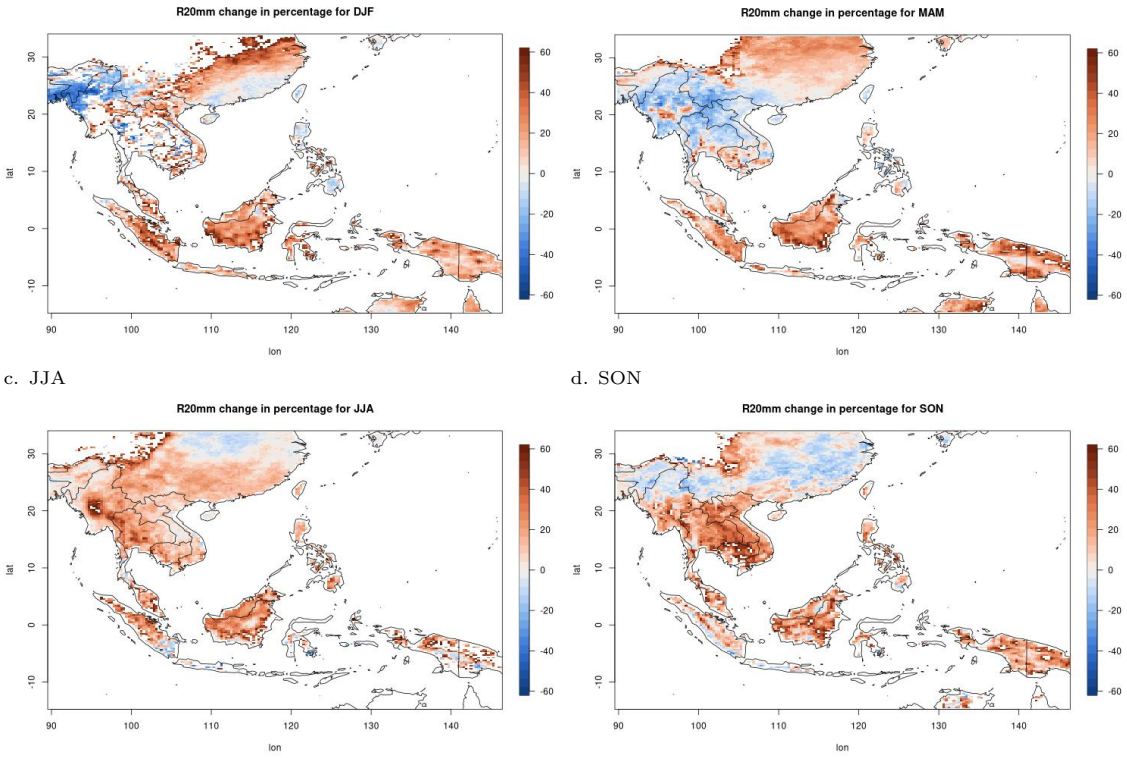

c. JJA

d. SON

Figure S9. Seasonal number of very heavy rainfall (R20mm) changes in percentage in the near future (2021-2050) compared to the historical period (1981-2010).

a. DJF

b. MAM

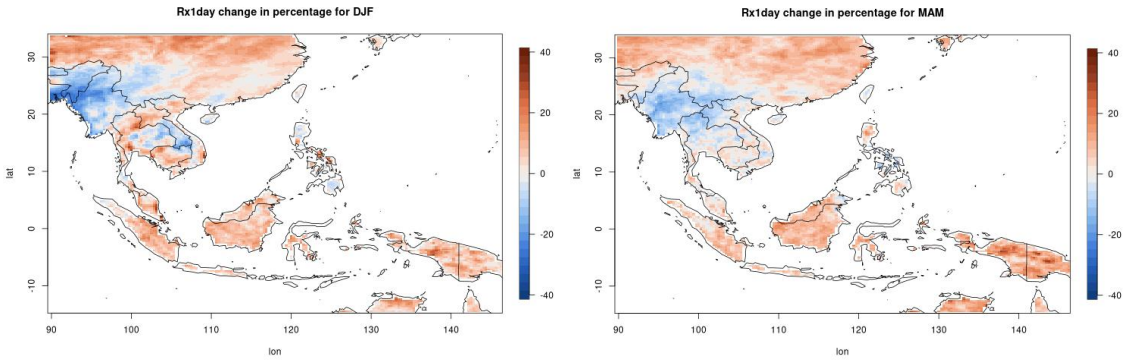

c. JJA

d. SON

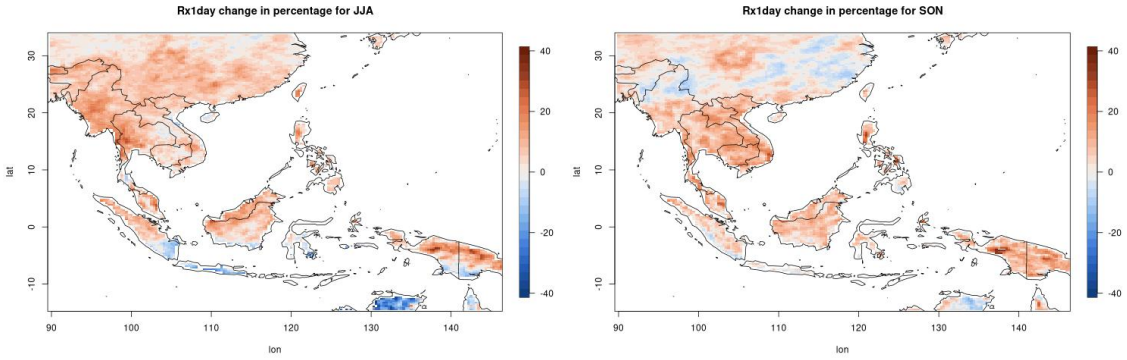

FIgure S10. Seasonal maximum daily rainfall (Rx1day) changes in percentage in the near future (2021-2050) compared to the historical period (1981-2010).

a. DJF

b. MAM

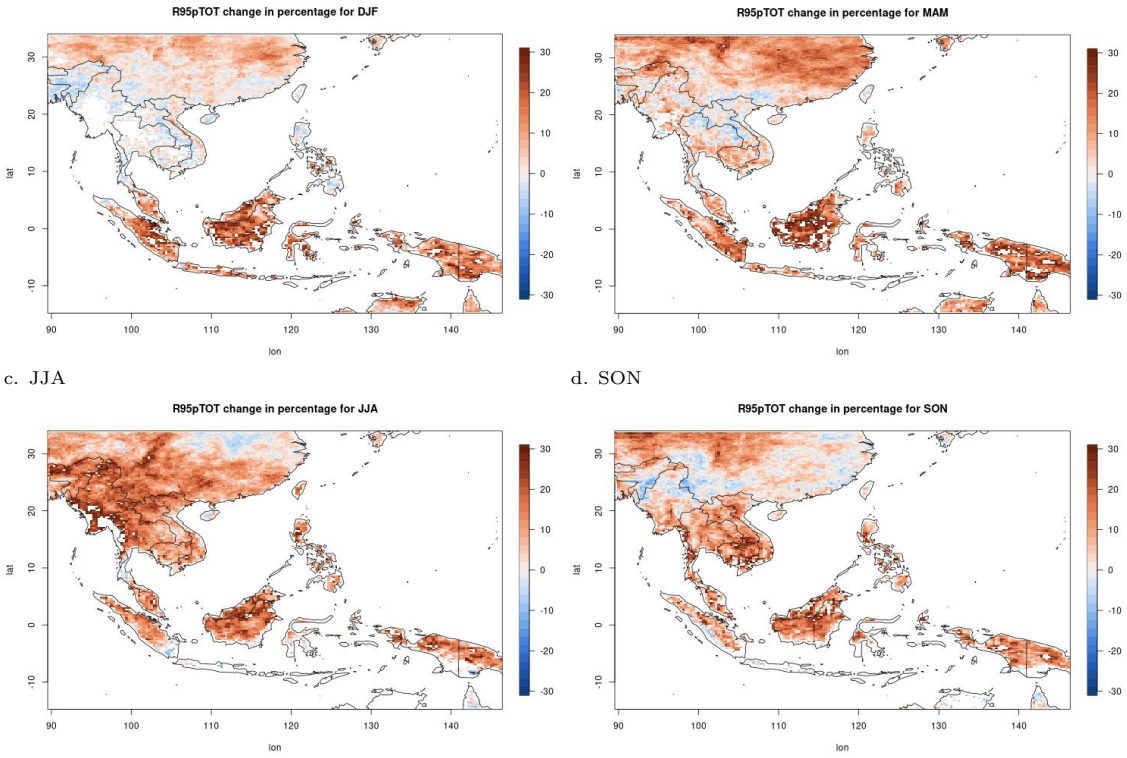

c. JJA

d. SON

Figure S11. Seasonal precipitation percent due to R95p days (R95pTOT) changes in percentage in the near future (2021-2050) compared to the historical period (1981-2010).

S12

Recession analysis is one of the methods for analysing the daily time series discharge to produce information about the low flow regime of a river.

Rivers with a slow recession rate are typically groundwater or lake-dominated, whereas a fast rate is characteristic of flashy rivers draining impermeable catchments with limited storage. The recession curve is modelled by fitting an analytical expression to the outflow function Q_t where Q is the rate of flow and t time. The time interval Δt is normally in the order of days. If Q_t is modelled as the outflow from a first-order linear storage with no inflow, the recession rate will follow the simple exponential equation:

$$Q_t = Q_0 \exp(-t/C)$$

where Q_t is the flow at time t; Q_0 is the flow at the start of the modelled recession period (t = 0); and C is the recession constant (dimension time).

We used recession analysis to calculate the recession constant (C). The C value is the overall recession rate in days. The calculation is used lfstat (https://rdrr.io/cran/lfstat/man/recession.html) r package which is based on the World Meteorological Organization (WMO) manual on low-flow estimation and prediction (Gustard and Demuth, 2009).

The individual recession segments (IRS) method with threshold level Q90 was used in the recession analysis. In the IRS method, the variability in individual recession segments is explicitly accounted for by fitting a recession model to each segment. Sample statistics of the model parameters, for example, the mean and variance of the recession constant, can subsequently be determined to characterize the overall recession behaviour of the catchment.

Figures a,b,c and d are the C values for rivers in the Mekong, the Sumatera-Peninsular Malaysia, Java and Borneo regions. The black boxes over Sumatera (Fig S13b) show the location of the Kampar (top) and Batang Hari (bottom) Rivers. In comparison, the black box over Java (Fig S13c) shows the location of part of the Bengawan Solo River.

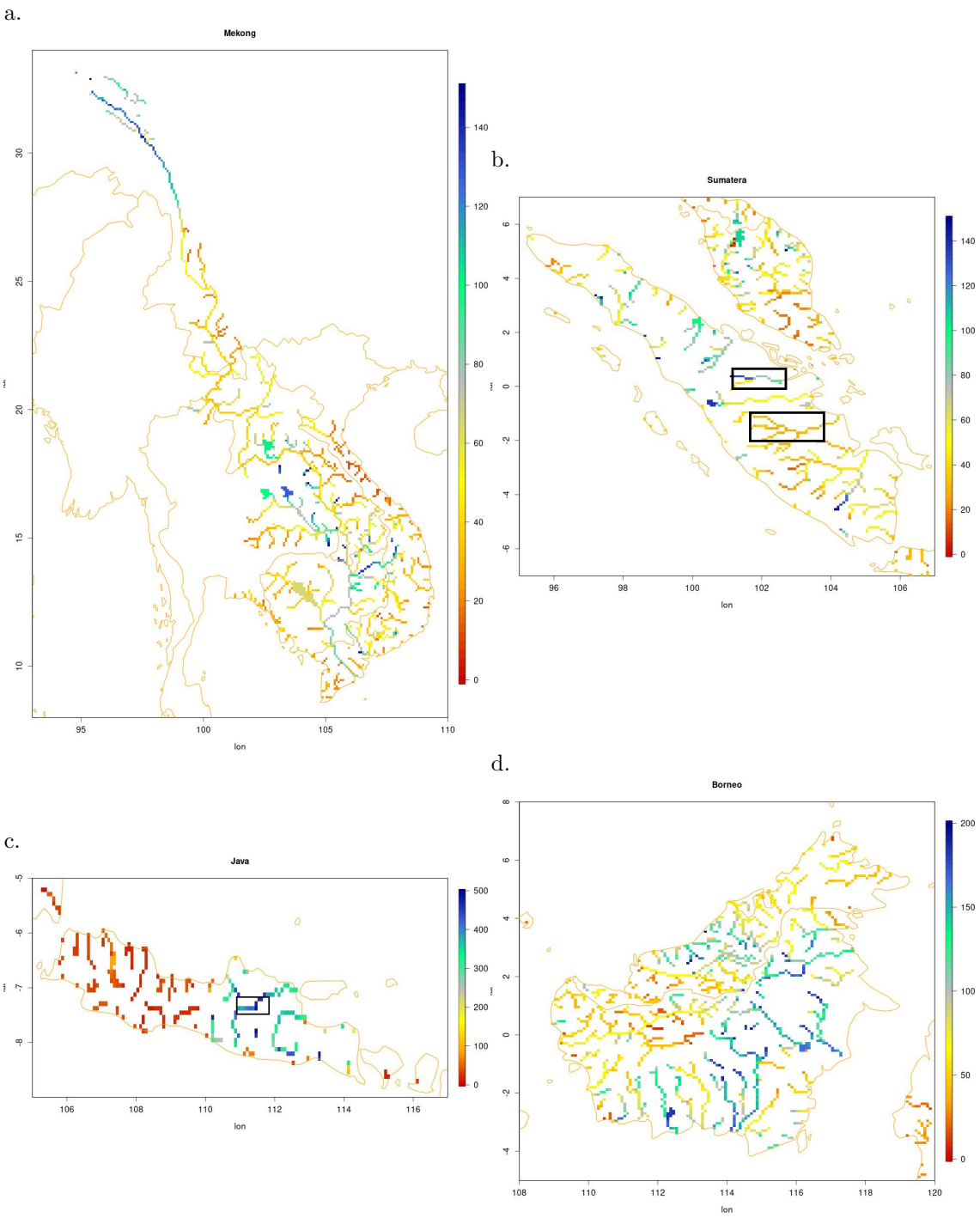

Figure S12. Recession constant (C) for (a) Mekong, (b) Sumatra island, (c) Java island and (d) Borneo.

S13

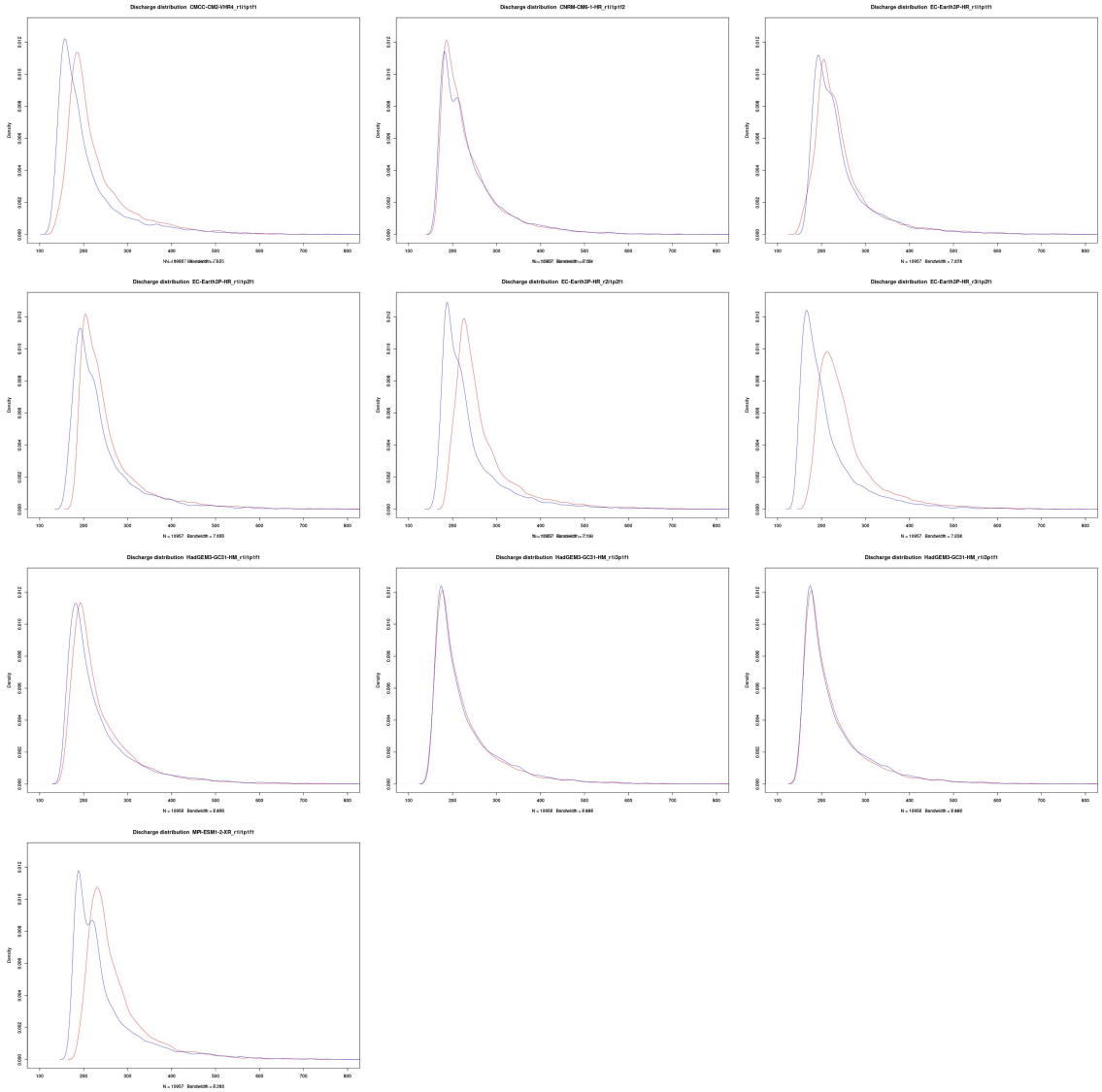

Figure S13a. Discharge distribution of Bengawan Solo River (relatively high C value)

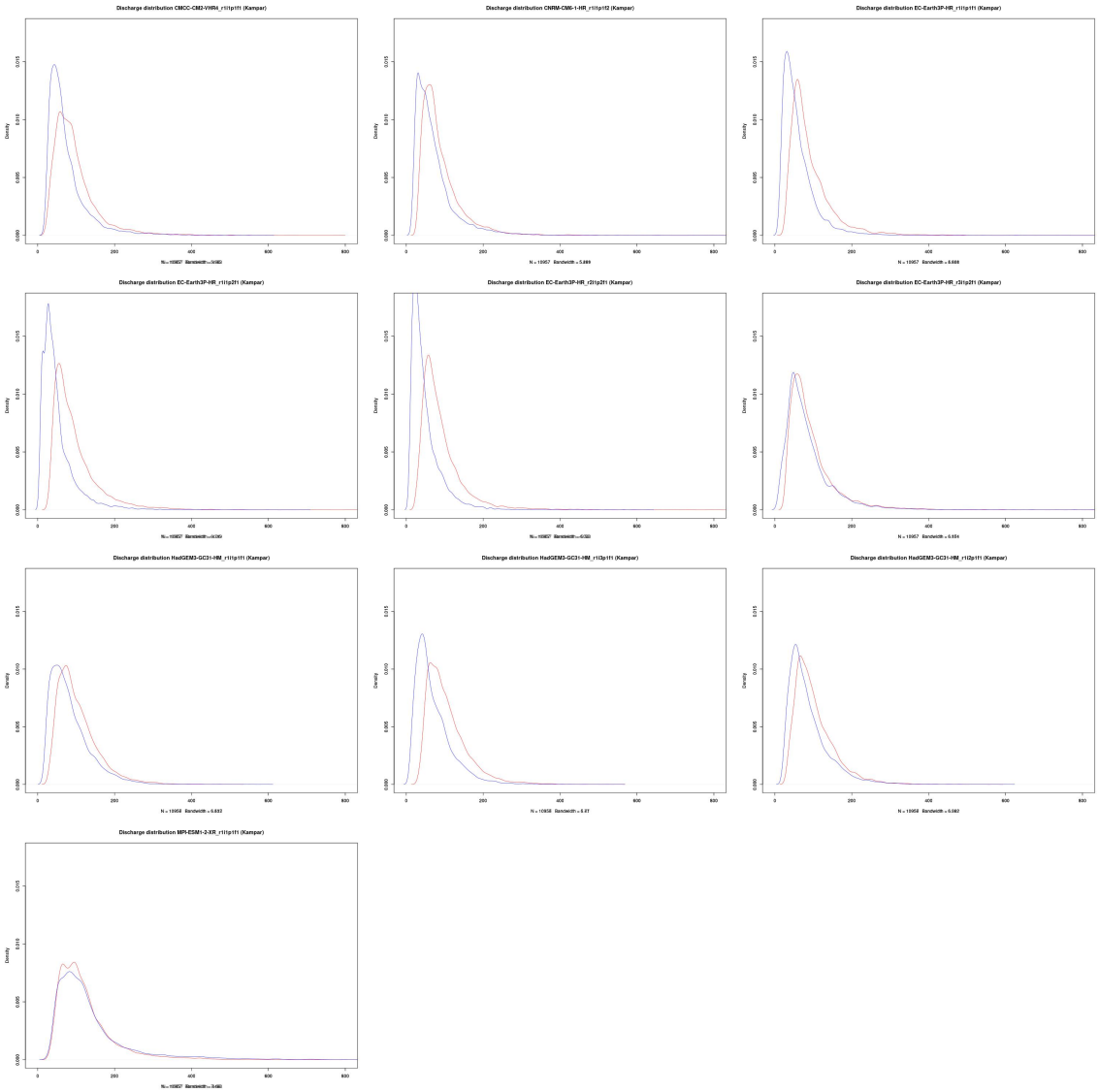

Figure 13b. Discharge distribution of Kampar River (relatively high C value)

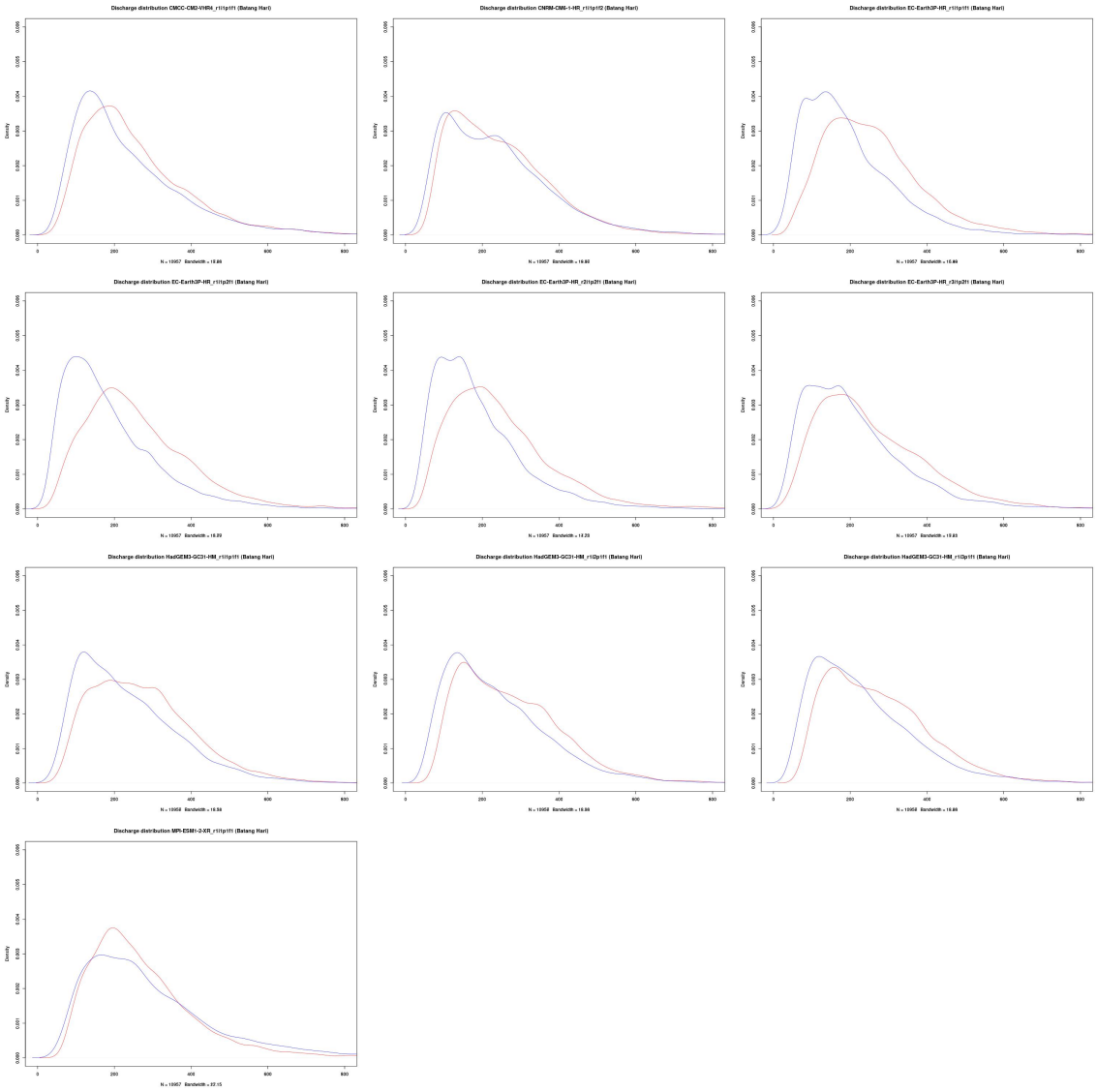

Figure 13c. Discharge distribution of Batang Hari River (relatively low C value)

References

Gustard, A. and Demuth, S.: Manual on low-flow estimation and prediction. Operational hydrology report, No. 50 WMO-No. 1029, World Meteorological Organization, Geneva, Switzerland, 136, 2009.